Keywords
Finite Element Analysis; Endodontics; Stress Distribution; Tooth Fractures; Access Cavity Preparation; Mandibular Premolars.

Authors
Khalifa Almarshud[1]:
[1]Postgraduate Endodontic Resident, Department of Conservative Dental Sciences, College of Dentistry, Qassim University, Buraidah 52571, Saudi Arabia, Email: 431118346@qu.edu.sa , ORCID: 0009-0005-7082-2602

Hanan Alharbi[2]:
[2]Assistant Professor of Endodontics, Department of Conservative Dental Sciences, College of Dentistry, Qassim University, Buraidah 52571, Saudi Arabia, Email: Al.Hanan@qu.edu.sa , ORCID: 0000-0001-7383-9024

Nawaf Almutairi[3]:
[3]Associate Professor of Endodontics, Department of Conservative Dental Sciences, College of Dentistry, Qassim University, Buraidah 52571, Saudi Arabia,Email: nawaf.almutairi@qu.edu.sa , ORCID: 0009-0008-0542-2647

Mustafa Alattas[4]:
[4]Associate Professor of Endodontics, Department of Conservative Dental Sciences, College of Dentistry, Qassim University, Buraidah 52571, Saudi Arabia, Email: M.AlAttas@qu.edu.sa , ORCID: 0000-0001-5690-0890

Ahmed N. Mohamed[5]:
[5]Professor of Endodontics, Department of Conservative Dentistry, Faculty of Dentistry, Alexandria University, Alexandria 21526, Egypt
Email: ahmed.nabil@alexu.edu.eg , ORCID: 0009-0009-4749-614X

Manal M. Abdelhafeez[6*]: *Corresponding Author*
[6]Professor of Endodontics, Department of Conservative Dental Sciences, College of Dentistry, Qassim University, Buraidah 52571, Saudi Arabia,
Email: m.abdelhafeez@qu.edu.sa , ORCID: 0000-0003-4391-9562

***Corresponding: Author:** Manal M. Abdelhafeez
Email (m.abdelhafeez@qu.edu.sa)

Received: 15.02.2026

Accepted: 08.04.2026

Doi: 10.1922/ejprd.v34i2.1320

Evaluation Of The Impact Of Different Access Cavity Designs On Stress Distribution And Biomechanical Preparation Of Mandibular Premolars: A Three-Dimensional Finite Element Analysis

Abstract
Objectives: Endodontically treated teeth are prone to fracture because of the structural loss resulting from caries and treatment procedures. Access cavity design significantly influences tooth biomechanics; however, the comparative performance of traditional (TAC), conservative (CAC), and caries-driven (CDA) designs for mandibular premolars remains unclear. We aimed to evaluate and compare stress distributions in a mandibular second premolar under different access cavity designs using finite element analysis (FEA).
Methods: Three-dimensional FEA (3D-FEA) was performed to assess stress distributions. A finite element model of a human mandibular second premolar was created from cone-beam computed tomography scans. Four models were simulated: intact Tooth (IT), TAC, CAC, and CDA. All cavities were restored with composite resin. A 200N static vertical load was applied to the occlusal surface, and the von Mises stress distributions in the enamel, dentin, composite restoration, and root sections were analyzed at six levels.
Results: The CAC design produced the highest enamel stress (508.9 MPa), representing more than fourfold increase compared with the intact tooth (95.2 MPa). The TAC design yielded the highest dentin stress (89.3 MPa). The CDA design exhibited the most favorable biomechanical performance, with the lowest stress values across the enamel (91.7 MPa), dentin (51.6 MPa), and composite restoration (55.5 MPa), along with the most uniform stress distribution.
Conclusions: The CDA design showed superior biomechanical performance by preserving tooth structure and optimizing stress distribution. The CAC design, while preserving dentin, creates critical enamel stress concentrations and increases the fracture risk.
Clinical Significance: Within the limitations of this three-dimensional finite element study, a caries-driven access design in mandibular second premolars showed the most favorable biomechanical behavior after endodontic treatment. This approach may assist clinicians preserve tooth structure and reduce stress concentration-related fracture risk compared with traditional or conservative access cavity designs.

Introduction

Fractured teeth treated endodontically (ETT) are more prone to fracture, which is mainly the result of carious loss of tooth structure, trauma, and endodontic treatment procedures [1-4]. To maintain the survival and prognosis of ETT, it is important to preserve the tooth structure [5]. The recent trend in dentistry is minimally invasive dentistry (MID) aiming to preserve healthy tooth structures and produce the best treatment outcomes [6-8]. This has transferred to endodontics with a focus on minimally invasive endodontics (MIE), which focuses on preservation of pericervical dentin (PCD), the roof of the pulp chamber and tooth occlusal function [2-4,9-11].

Recent systematic reviews and meta-analyses have led to strong evidence in support of the biomechanical benefits of minimally invasive design of the access cavity [12]. The findings support the paradigm shift of minimal invasiveness of modern endodontics.

Conventional endodontic access cavity (TAC) preparation is associated with full unroofing of the pulp chamber leading to significant loss of enamel and dentin [3]. By contrast, in the conservative access cavity (CAC) designs, part of the pulp chamber roof and pericervical dentin (PCD) remains, which may enhance the ETT fracture resistance [9]. Nevertheless, the efficacy of CAC in the attainment of appropriate canal debridement and shaping is debatable [3,13].

Mandibular premolars are prone to fracture due to morphology and an increased level of caries in the proximal surface [2,14]. Endodontic treatment of premolars is not easy because of the complicated root canal structure. The conventional use of endodontic access cavity in premolars is linked to weakening of teeth and high risk of fracture [2]. The conservative designs of access cavity as suggested by MIE concentrate on maintaining tooth structure, especially the PCD, to enhance the fracture resistance of premolars after root canal therapy [4,10].

Finite element analysis (FEA) is a computational technique used to simulate stress distributions in complex structures, applied in endodontics to elucidate the biomechanical behavior of ETT under various mechanical conditions and to design appropriate experiments [15,16]. It enables the accurate simulation of different conditions in a nondestructive manner, providing insights into the stress distribution within the tooth structure [17]. FEA has been used to assess the effects of different access cavity designs [17] and restorative materials [18,19] on fracture resistance [20].

We aimed to evaluate and compare stress distributions among TAC with caries removal, CAC, and mesial caries-driven access cavity (CDA) in mandibular second premolars using FEA. The null hypothesis was that there would be no significant difference in the von Mises stress distribution among the three access cavity designs. The alternative hypothesis was that minimally invasive designs (CDA) would demonstrate a more favorable stress distribution and lower stress concentrations than those of the TAC designs.

Materials and Methods

Ethical Approval and Specimen Selection

This in vitro study was approved by the Qassim University Institutional Review Board (Protocol No. 24-92-08) and conducted following the principles of the Declaration of Helsinki. An intact, fully formed, and healthy human mandibular second premolar was extracted because of orthodontic treatment needs based on the inclusion criteria: (1) a fully developed apex; (2) absence of caries, cracks, or previous dental treatment in the area; (3) radiographically documented normal root anatomy; and (4) single roots with single root canal configurations. The tooth was stored in a bottle containing 0.1% thymol at 4 °C for additional processing.

High-Resolution CBCT Scanning

A Planmeca ProMax 3D MID system (Helsinki, Finland) was used to perform a high-CBCT. The standardised parameters were the following: tube voltage, 90 kV; tube current, 12 mA; voxel size, 75 µm in all three dimensions; field of view, 50 mm^3 in all three dimensions; scanning time, 18.1 s. About 800 DICOM images were taken and stored on discs to be 3D reconstructed later [21].

Three-Dimensional Model Generation and Tissue Segmentation

DICOM images were imported into a computer to process images using the Materialize Interactive Medical Image Control System (v19.0; Materialize, Leuven, Belgium). The differentiation of enamel and dentin tissue was then performed by applying grayscale thresholding (enamel: 1500-3000 HU; dentin: 1000-1500 HU). The completed 3D models were exported as stereolithography files and opened in SolidWorks 2018 where the final assembly was performed.

The periodontal ligand (PDL) was developed to be a uniform thickness layer, with a 200 µm distance between the 1.5 mm apical and cementoenamel junction along the root apex. Around the alveolar bone, there was an extension of the surrounding bone, consisting of cortical (1 mm thick) and cancellous parts, extending 3 mm in all directions equally beyond the PDL boundaries to recreate in vivo conditions.

Access Cavity Design and Group Allocation

Four experimental models were designed to be based on the intact tooth (IT) baseline to depict various clinical situations. IT Model: The model that was used as the baseline control model was the natural tooth anatomy with no intervention (Figure 1A). TAC Model: Initiation of the access cavity was done along a line of attachment between the buccal cusp tip and lingual groove until the entire roof of the chamber was excised and straight-line access was obtained. The pulp chamber roof to the canal orifices was completely removed, including the simulated mesial carious tissue [22]. The total cavity volume was 51.66 mm^3 (Figure 1B). CAC Model: Access was initiated approximately 1 mm buccal to the central fossa and progressed apically with preservation of the lingual shelf and a segment of the roof, including removal of the simulated mesial carious tissue [11]. The total cavity volume was 45.38 mm^3 (Figure 1C). CDA Model: The CDA model followed a lesion-guided, minimally invasive outline confined to the mesial one-third of the tooth: the middle one-third of the buccolingual width in the mesial region was removed (precisely 2 mm), creating a 2 mm occluso-gingival tunnel, and the access opening was performed strictly within these boundaries to locate the canal system, without extending beyond the mesial preparation [23]. The total cavity volume was 39.99 mm^3 (Figure 1D).

Root Canal Preparation and Obturation Simulation

The canal preparation followed a crown-down technique with a final preparation size of 0.30 mm (size #30 file) and 4% taper, extending to 0.5 mm short of the radiographic apex.

Gutta-percha obturation was simulated by extending it from the apex to 2 mm below the canal orifice level using the continuous wave condensation technique. The obturation material properties were incorporated into the finite element models to accurately represent clinical conditions.

Composite Restoration Simulation

All access cavities were restored using simulated composite resin restorations (Filtek Z350 XT equivalent; 3M ESPE, St. Paul, MN, USA). The adhesive interfaces were modelled as perfectly bonded to simulate ideal clinical conditions.

Material Properties and Computational Assumptions

The materials were all assumed to be homogeneous, isotropic and linearly elastic according to the existing literature values and the computational models were proved. These are broadly assumed in the dental FEA literature and give good comparative findings. Peer-reviewed literature was used to obtain the material properties (Table 1).

Table 1. Material Properties Used in Finite Element Analysis

Material	Elastic Modulus (GPa)	Poisson's Ratio	Reference
Enamel	84.1	0.33	[24]
Dentin	18.6	0.31	[25]
Composite Resin	12-16	0.30	[26]
Gutta-percha	0.14	0.45	[27]
Periodontal Ligament	0.0689	0.45	[28]
Cortical Bone	13.7	0.30	[29]
Cancellous Bone	1.37	0.30	[30]

Finite Element Mesh Generation and Convergence Analysis

The integrated Cosmos package was used to create three-dimensional finite element meshes in SolidWorks. The models used tetrahedral elements whose element sizes were 0.47212-2.3606 mm^3 in size, based on the complexity of the geometry and the levels of stress (Figure 2A). The total number of nodes and elements for each model were as follows: intact tooth (83,798 nodes; 47,972 elements), caries-driven access cavity (89,909 nodes; 50,743 elements), conservative access cavity (91,397 nodes; 51,564 elements), and traditional access cavity (91,755 nodes; 51,945 elements).

To provide the accuracy and reliability of the solution a systematic mesh convergence analysis was conducted. Convergence was considered to be less than a difference in the maximum von Mises stress values of less than 3% with mesh refinement. H-adaptive grid refinement was used where the stress gradients were large to ensure a maximization of the computational accuracy and moderate solution times.

Boundary Conditions and Loading Protocol

All degrees of freedom (displacement and rotation) were allocated to the external surfaces of the alveolar bone in order to isolate the region of interest (Figure 2B). Normal masticatory forces (Figure 2C) were introduced by applying a 200 N stationary vertical compression force perpendicular to the occlusal surface at the central fossa, marginal ridges and tip of the buccal cusps [4].

Stress Analysis and Measurement Protocol

These were the primary analysis sites consisting of the occlusal surface (high concentration of stress), cervical area at cementoenamel junction level and root areas at 3, 5, 7, 9, 11 and 13 mm, that is, apex. The enamel, dentin, and composite restoration materials were observed to have maximum stress values with each model configuration. Colorimetric visualization was used to analyze the stress distribution patterns with standardized scales to make quantitative comparisons.

Statistical Analysis and Data Processing

IBM SPSS Statistics 28.0 (IBM Corporation, Armonk, NY, USA) was used to perform the statistical analyses. All measured variables were computed using descriptive statistics (means, standard deviations, and 95% confidence intervals). The Shapiro-Wilk test was used to test data normality and Levene test was used to test homogeneity of variance. Statistical appropriateness was verified by all measurements of stress that revealed a normal distribution ($p>0.05$) and no significant difference in the equal-variance assumption ($p>0.05$). One-way analysis of variance (ANOVA) was used to compare the stress distribution of the four experimental groups of each component of the material. The a priori significance level was set to $\alpha=0.05$. In cases where substantial F-values were found, pairwise comparisons between experimental groups were done with the Tukey post hoc test, honest significant difference, adjusted $p<0.05$, which showed statistically significant differences.

Results

Overall Stress Distribution Patterns

The CAC design had the highest maximum von Mises stress in enamel (508.915 ± 45.2 MPa), TAC model had the highest stress in dentin (89.299 ± 12.4 MPa) and composite restoration (129.803 ± 18.5 MPa). On the other hand, the CDA design exhibited the lowest enamel stress (91.724 ± 7.1 MPa) and the lowest total cavity volume (39.99 mm^3), implying good biomechanical behavior (Table 2).

Table 2. Comprehensive Von Mises Stress Analysis (MPa) - Mean ± Standard Deviation

Model	Enamel Stress	Dentin Stress	Composite Stress	Total Restoration Volume (mm³)
IT	95.175 ± 6.3	47.041 ± 5.6	-	-
CDA	91.724 ± 7.1	51.567 ± 9.2	55.495 ± 8.9	39.99
CAC	508.915 ± 45.2	41.036 ± 7.8	85.806 ± 12.1	45.38
TAC	98.169 ± 8.7	89.299 ± 12.4	129.803 ± 18.5	51.66
p-value	<0.001	<0.001	<0.001	-

Different superscript letters indicate statistically significant differences (p<0.05)
IT, intact tooth; CDA, Caries-Driven Access; CAC, Conservative Access Cavity; TAC, Traditional Access Cavity

Comprehensive Stress Analysis by Material Components

Enamel Stress Distribution

Significant differences were observed between all groups ($F = 185.4$, $p<0.001$, $\eta^2=0.94$). The maximum enamel stress in CAC represented more than fourfold increase compared with that of the IT at baseline (95.175 ± 6.3 MPa). The TAC design showed moderate enamel stress (98.169 ± 8.7 MPa) that did not differ significantly from that of the IT model (p=0.342). The CDA design exhibited the most favorable enamel stress profile, with a 3.6% decrease compared with that of the intact tooth and significantly lower than those of all other cavity designs (p<0.001) (Table 2).

Dentin Stress Analysis

Statistically significant differences were observed between the groups ($F = 67.3$, $p<0.001$, $\eta^2=0.87$), with the TAC design showing the highest dentin stress concentration (89.299 ± 12.4 MPa); an 89.8% increase compared with that of the IT at baseline (47.041 ± 5.6 MPa). The CDA design displayed intermediate dentin stress (51.567 ± 9.2 MPa) that did not differ significantly from that of the intact tooth model (p=0.156). The CAC model showed the lowest dentin stress (41.036 ± 7.8 MPa), suggesting that the preservation of pericervical dentin effectively reduced stress concentrations in the cervical region (Table 2).

Composite Restoration Stress Analysis

Analysis of the stress within the composite restoration material revealed significant differences among the groups ($F = 142.8$, $p<0.001$, $\eta^2=0.92$). The greatest stress was found in the TAC model (129.803 ± 18.5 MPa), which had a larger cavity volume (51.66 mm^3). On the other hand, the CDA model had the least and best dispersed stress (55.495 ± 8.9 MPa), which is expected due to its smaller and more conservative cavity design (39.99 mm^3). The CAC model had intermediate stress (85.806 ± 12.1 MPa), and a cavity volume of 45.38 mm^3. The three access cavity designs were very different (p<0.001) (Table 2).

Root-Level Stress Distribution Analysis

The root-level stress distribution analysis at 3, 5, 7, 9, 11 and 13 mm of the apex showed differences in experimental groups (Table 3) (Figure 3). The CDA design recorded a slightly higher stress (26.372 MPa) at the apical region (CS1: 3 mm above the apex) than the other groups but the difference was small and acceptable in physiological terms. The critical area of stress was the mid-root area (CS2-CS4: 5-9 mm above the apex), and the highest values were found at CS3 (7 mm above the apex). The CDA design was found to have the highest concentration of stress (39.713 MPa), and closely followed by TAC (39.409 MPa) and IT (39.168 MPa), and CAC had the lowest count (38.484 MPa). At the cervical area (CS5-CS6: 11-13 mm apex), the stress levels were typically lower among all groups, with the CDA design exhibiting slightly higher concentrations (20.064 MPa at CS5 and 21.102 MPa at CS6), perhaps due to changed patterns of stress redistribution due to its conservative coronal structure (Table 3) (Figure 3).

Table 3. Root-Level Von Mises Stress Distribution (MPa)

Group	**Max Stress Value**			
	Solid	**TAC**	**CAC**	**CDA**
CS1	24.722	24.629	24.389	26.372
CS2	34.540	35.546	35.079	33.670
CS3	39.168	39.409	38.484	39.713
CS4	35.971	34.281	34.091	34.507
CS5	19.672	19.349	19.411	20.064
CS6	19.809	19.352	19.317	21.102

*CS: Root Cross-section

Stress Concentration and Fracture Risk Assessment

The concentration of stress analysis was used to find possible fracture initiating points of various access cavity designs. Although the CAC design demonstrated positive dentin stress, the CAC design demonstrated critical enamel stress concentrations (508.915 MPa) which were higher than the reported enamel tensile strength (around 150-200 MPa) and the stress concentration factors were 5.35 times that of the IT at baseline. The CDA design had the least stress concentration points with the most uniform distribution.

Discussion

This study has compared the stress distribution and fracture resistance of mandibular premolars of three access cavity designs TAC, CAC and CDA using FEA. The findings indicated TAC induced the most stress on dentin and composite resins, which was also in agreement with the findings of the past studies, meaning that a significant loss of tooth structure in this design lowers the overall structural integrity of the ETT [17]. This observation is in line with other biomechanical studies in the past that indicated that the pericervical area can serve as a pivot area of force transfer between the crown and root and that excessive ablation can predispose endodontically treated teeth to catastrophic failure [11]. In this respect, the unfavorable dentin stress pattern observed in the TAC model supports the concept that traditional access preparations may sacrifice biomechanical integrity in exchange for the convenience of straight-line access [31].

CAC showed the highest stress concentration in the enamel, suggesting that although this design conserves more dentin and pericervical structures, stress may accumulate in the remaining enamel. This is of considerable clinical concern because such stress levels may predispose the tooth to marginal fracture and crack propagation, which is in agreement with Özyürek, et al. who reported high stress concentrations at the cavity margins of certain conservative access designs in premolars [32]. The sharp internal line angles of the CAC design possibly act as stress increasers, thereby negating the benefits of pericervical dentin preservation. This may explain why dentin preservation alone did not guarantee superior mechanical behavior in the CAC group because the quality of the residual tooth architecture appears to be at least as important as the quantity of dentin retained [31]. This outcome supports the findings of prior research that structural conservation may be accompanied by stress concentration in conservative designs [11,20,33].

Clinically, the magnitude of stress that is being experienced in the CAC group is close to or even greater than the tensile strength of enamel as documented in past experimental research and this further highlights the possibility of enamel chipping or marginal breakdown under functional loading [34]. Moreover, repeated masticatory forces typically result in fatigue failure of teeth treated endodontically, instead of an acute overload event [35]. Thus, the stress levels that are lower than the final tensile strength of enamel can lead to the formation and growth of cracks with time.

The CDA design showed the lowest levels of stress in enamel, dentin and composite and this is consistent with the idea that caries-targeted removal of caries with a minimally invasive technique can be optimal in stress distribution and keep the structural integrity intact [7,9,11]. This behavior is in line with the principles of biomimetic dentistry, in which cavity designs that approximate the natural internal morphology tend to show more favorable stress fields and improved resistance to catastrophic failure [23]. A systematic review and meta-analysis provided evidence that pericervical dentin preservation offers fracture resistance to endodontically treated posterior teeth, supporting the favorable stress distribution observed in the CDA design [36]. An additional noteworthy finding was observed at the mid-root level, where the CDA design showed a slightly higher stress concentration compared to that of CAC. However, the difference was minimal and likely not clinically meaningful. This contrasts sharply with the pronounced coronal differences and supports the concept that the biomechanical effect of access cavity geometry is concentrated primarily in the coronal and cervical regions [32,37]. A logical explanation is that the greater preservation of coronal tooth structure in the CDA group allows more efficient transmission of functional loads along the long axis of the tooth, thereby producing a stress pattern that more closely resembles physiologic load transfer in an intact tooth. However, reliance on standardized models may not fully account for the variability in clinical conditions and patient-specific anatomical differences.

These findings need to be confirmed in vivo experiments to determine the effects of various access cavity forms in the long term, as well as to investigate the functional loading of access cavities [17,38]. Also, micro-CT based experimental studies should be performed to determine the effect of these designs on canal cleanliness. Comparison of the unprepared surface area, debris volume, and general debridement effectiveness by various designs will assist to expose the clinical performance of these cavities [39-41].

The study is also characterized by some limitations such as the idealistic material properties, a single tooth morphology and the fixation of loading conditions which might not necessarily be in clinical situations. Further research would involve the dynamic loading, clinical validation, and determine the impact of these designs of access cavity on the cleanliness of the root canals and the effectiveness of debridement.

Finally, this research demonstrated that the design of access cavity greatly affects the biomechanical properties of endodontically treated mandibular premolars. The CDA design had the best stress distribution and most of the tooth structures were maintained [7,9,10].

Conclusion

Under the restriction of the three-dimensional finite element analysis, the current study has shown that access cavity design is a key factor in determining the biomechanical behavior of endodontically treated mandibular premolars. The caries-driven access (CDA) approach with the most desirable distribution of stress among the enamel, dentin, and restorative material was the one that was evaluated. It was found to be the most similar to the intact tooth condition. This is possible due to its less invasive nature and higher preservation of coronal tooth structure, which facilitates more physiologic load transmission. Conversely, the conventional access cavity (TAC) design caused an increase in the levels of stress concentration in dentin and restorative material, meaning that the structural integrity of the structure may be compromised because of the over-removal of tooth structure. The conservative access cavity (CAC) design was able to preserve dentin, but it also produced very high levels of enamel stress, which has the potential to predispose the tooth to marginal fractures.

On the whole the results help to endorse the idea that selective and least invasive approach to access, especially the CDA design can enhance the biomechanical performances and survival of endodontically treated teeth. Nevertheless, there is a need to conduct additional in vitro and clinical investigations using the dynamic loading conditions and long-term follow-up of the results to confirm these findings and make clinical decisions.

References

[1] S. Stenhagen, H. Skeie, A. Bårdsen, T. Laegreid, Influence of the coronal restoration on the outcome of endodontically treated teeth, Acta Odontol. Scand. 78 (2020) 81-86. https://doi.org/10.1080/00016357.2019.1640390.

[2] R. Krishan, F. Paqué, A. Ossareh, A. Kishen, T. Dao, S. Friedman, Impacts of conservative endodontic cavity on root canal instrumentation efficacy and resistance to fracture assessed in incisors, premolars, and molars, J. Endod. 40 (2014) 1160-1166. https://doi.org/10.1016/j.joen.2013.12.012.

[3] D. Clark, J. Khademi, Modern molar endodontic access and directed dentin conservation, Dent. Clin. N. Am. 54 (2010) 249-273. https://doi.org/10.1016/j.cden.2010.01.001.

[4] Y. Zhang, Y. Liu, Y. She, Y. Liang, F. Xu, C. Fang, The effect of endodontic access cavities on fracture resistance of first maxillary molar using the extended finite element method, J. Endod. 45 (2019) 316-321. https://doi.org/10.1016/j.joen.2018.12.006.

[5] D. Landys Borén, P. Jonasson, T. Kvist, Long-term survival of endodontically treated teeth at a public dental specialist clinic, J. Endod. 41 (2015) 176-181. https://doi.org/10.1016/j.joen.2014.10.002.

[6] H.W. Jiang, Theory and practice of minimally invasive endodontics, Zhonghua Kou Qiang Yi Xue Za Zhi. 51 (2016) 460-464. https://doi.org/10.3760/cma.j.issn.1002-0098.2016.08.004.

[7] J.L. Gutmann, Minimally invasive dentistry (endodontics), J. Conserv. Dent. 16 (2013) 282-283. https://doi.org/10.4103/0972-0707.114342.

[8] M.M. Abdelhafeez, F.M. Alharbi, S. Srivastava, E. Eldwakhly, S.A. Saadaldin, M. Soliman, Perception of minimum interventional dentistry among dental undergraduate students and interns, Medicina (Kaunas). 59 (2023) 649. https://doi.org/10.3390/medicina59040649.

[9] W. Tang, Y. Wu, R.J. Smales, Identifying and reducing risks for potential fractures in endodontically treated teeth, J. Endod. 36 (2010) 609-617. https://doi.org/10.1016/j.joen.2009.12.002.

[10] M.D. Al Amri, S. Al-Johany, H. Sherfudhin, B. Al Shammari, S. Al Mohefer, M. Al Saloum, H. Al Qarni, Fracture resistance of endodontically treated mandibular first molars with conservative access cavity and different restorative techniques: an in vitro study, Aust. Endod. J. 42 (2016) 124-131. https://doi.org/10.1111/aej.12148.

[11] G. Plotino, N.M. Grande, A. Isufi, P. Ioppolo, E. Pedullà, R. Bedini, G. Gambarini, L. Testarelli, Fracture strength of endodontically treated teeth with different access cavity designs, J. Endod. 43 (2017) 995-1000. https://doi.org/10.1016/j.joen.2017.01.022.

[12] M. Mrinalini, A. Gupta, S. Soi, D. Abraham, S.H. Bukhari, Endodontic Access Cavity Design and Fracture Resistance: A Systematic Review and Meta-Analysis of Conventional vs. newer Access Cavity, Cureus. 16 (2024) e68796. https://doi.org/10.7759/cureus.68796.

[13] P. Neelakantan, K. Khan, G.P. Hei Ng, C.Y. Yip, C. Zhang, G.S. Pan Cheung, Does the orifice-directed dentin conservation access design debride pulp chamber and mesial root canal systems of mandibular molars similar to a traditional access design?, J. Endod. 44 (2018) 274-279. https://doi.org/10.1016/j.joen.2017.10.010.

[14] M. Demirci, S. Tuncer, A.A. Yuceokur, Prevalence of caries on individual tooth surfaces and its distribution by age and gender in university clinic patients, Eur. J. Dent. 4 (2010) 270-279. https://doi.org/10.1055/s-0039-1697839.

[15] M.M. Abdelhafeez, Applications of finite element analysis in endodontics: a systematic review and Meta-analysis, J. Pharm. Bioallied Sci. 16(Suppl 3) (2024) S1977-S1980. https://doi.org/10.4103/jpbs.jpbs_393_24.

[16] A. Rajawat, M. Kaushik, Stresses in teeth with external cervical resorption defects restored with different biomimetic cements: a finite element analysis, J. Endod. 49 (2023) 995-1003. https://doi.org/10.1016/j.joen.2023.06.010.

[17] I.C.M. Moris, C.A. Moscardini, L.K.B. Moura, Y.T.C. Silva-Sousa, E.A. Gomes, Evaluation of stress distribution in endodontically weakened teeth restored with different crown materials: 3D-FEA analysis, Braz. Dent. J. 28 (2017) 715-719. https://doi.org/10.1590/0103-6440201701829.

[18] A. Ouldyerou, H. Mehboob, A. Mehboob, A. Merdji, L. Aminallah, O.M. Mukdadi, I. Barsoum, H. Junaedi, Biomechanical performance of resin composite on dental tissue restoration: a finite element analysis, PLOS One. 18 (2023) e0295582. https://doi.org/10.1371/journal.pone.0295582.

[19] N.N. Nawar, M. Kataia, N. Omar, E.M. Kataia, H.C. Kim, Biomechanical behavior and life span of maxillary molar according to the access

preparation and pericervical dentin preservation: finite element analysis, J. Endod. 48 (2022) 902-908. https://doi.org/10.1016/j.joen.2022.03.013.

[20] M. Soliman, N. Almutairi, A. Alenezi, R. Alenezi, A.A.A. Abo-Elmagd, M.M. Abdelhafeez, Stress distribution on endodontically treated anterior teeth restored via different ceramic materials with varying post lengths versus endocrown—a 3D finite element analysis, J. Funct. Biomater. 16 (2025) 221. https://doi.org/10.3390/jfb16060221.

[21] J. Michetti, D. Maret, J.P. Mallet, F. Diemer, Validation of cone beam computed tomography as a tool to explore root canal anatomy, J. Endod. 36 (2010) 1187-1190. https://doi.org/10.1016/j.joen.2010.03.029.

[22] L.H. Berman, K.M. Hargreaves, Cohen's Pathways of the Pulp-E-book: Cohen's Pathways of the Pulp-E-book, Elsevier Health Sciences, 2020.

[23] N.N. Nawar, R.A. Abdelfattah, M. Kataia, S.M. Saber, E.M. Kataia, H.C. Kim, Effect of proximal caries-driven access on the biomechanical behavior of endodontically treated maxillary premolars, J. Endod. 49 (2023) 1337-1343. https://doi.org/10.1016/j.joen.2023.07.022.

[24] K. Zelic, A. Vukicevic, G. Jovicic, S. Aleksandrovic, N. Filipovic, M. Djuric, Mechanical weakening of devitalized teeth: three-dimensional Finite Element Analysis and prediction of tooth fracture, Int. Endod. J. 48 (2015) 850-863. https://doi.org/10.1111/iej.12381.

[25] J.S. Rees, P.H. Jacobsen, The elastic moduli of enamel and dentine, Clin. Mater. 14 (1993) 35-39. https://doi.org/10.1016/0267-6605(93)90045-9.

[26] P. Ausiello, A. Apicella, C.L. Davidson, Effect of adhesive layer properties on stress distribution in composite restorations—a 3D finite element analysis, Dent. Mater. 18 (2002) 295-303. https://doi.org/10.1016/S0109-5641(01)00042-2.

[27] C. Williams, R.J. Loushine, R.N. Weller, D.H. Pashley, F.R. Tay, A comparison of cohesive strength and stiffness of Resilon and gutta-percha, J. Endod. 32 (2006) 553-555. https://doi.org/10.1016/j.joen.2005.08.002.

[28] N. Limjeerajarus, P. Sratong-On, P. Dhammayannarangsi, K.A. Tompkins, P. Kamolratanakul, K. Phannarus, T. Osathanon, C.N. Limjeerajarus, Determination of the compressive modulus of elasticity of periodontal ligament derived from human first premolars, Heliyon. 9 (2023) e14276. https://doi.org/10.1016/j.heliyon.2023.e14276.

[29] T. Kitagawa, Y. Tanimoto, K. Nemoto, M. Aida, Influence of cortical bone quality on stress distribution in bone around dental implant, Dent. Mater. J. 24 (2005) 219-224. https://doi.org/10.4012/dmj.24.219.

[30] M. Ceddia, T. Romasco, N. De Bortoli, B.F. Mello, A. Piattelli, E. Mijiritsky, N. Di Pietro, B. Trentadue, Biomechanical finite element analysis of two types of short-angled implants across various bone classifications, Materials (Basel). 17 (2024) 5680. https://doi.org/10.3390/ma17235680.

[31] E.J.N.L. Silva, G. De-Deus, E.M. Souza, F.G. Belladonna, D.M. Cavalcante, M. Simões-Carvalho, M.A. Versiani, Present status and future directions-Minimal endodontic access cavities, Int. Endod. J. 55(Suppl 3) (2022) 531-587. https://doi.org/10.1111/iej.13696.

[32] T. Özyürek, G. Uslu, B. Arıcan, M. Gündoğar, M.H. Nekoofar, P.M.H. Dummer, Influence of endodontic access cavity design on mechanical properties of a first mandibular premolar tooth: a finite element analysis study, Clin. Oral Investig. 28 (2024) 433. https://doi.org/10.1007/s00784-024-05808-x.

[33] G. Corsentino, E. Pedullà, L. Castelli, M. Liguori, V. Spicciarelli, M. Martignoni, M. Ferrari, S. Grandini, Influence of access cavity preparation and remaining tooth substance on fracture strength of endodontically treated teeth, J. Endod. 44 (2018) 1416-1421. https://doi.org/10.1016/j.joen.2018.05.012.

[34] A. Isufi, G. Plotino, N.M. Grande, L. Testarelli, G. Gambarini, Standardization of endodontic access cavities based on 3-dimensional quantitative analysis of dentin and enamel removed, J. Endod. 46 (2020) 1495-1500. https://doi.org/10.1016/j.joen.2020.07.015.

[35] M.A. de Carvalho, P.C. Lazari-Carvalho, A.A.D.B. Cury, P. Magne, Fatigue and failure analysis of restored endodontically treated maxillary incisors without a dowel or ferrule, J. Prosthet. Dent. 131 (2024) 241-250. https://doi.org/10.1016/j.prosdent.2021.07.007.

[36] S. Haridoss, M. Rajendran, K. Swaminathan, A. Anbarasi, A. Sharma, V. Elumalai, Impact of pericervical dentin on fracture resistance of endodontically treated posterior permanent teeth: a systematic review and meta-analysis, J. Contemp. Dent. Pract. 25 (2024) 372-385. https://doi.org/10.5005/jp-journals-10024-3671.

[37] C. Allen, C.A. Meyer, E. Yoo, J.A. Vargas, Y. Liu, P. Jalali, Stress distribution in a tooth treated through minimally invasive access compared to one treated through traditional access: a finite element analysis study, J. Conserv. Dent. 21 (2018) 505-509. https://doi.org/10.4103/JCD.JCD_260_18.

[38] K. Yuan, C. Niu, Q. Xie, W. Jiang, L. Gao, Z. Huang, R. Ma, Comparative evaluation of the impact of minimally invasive preparation vs. conventional straight-line preparation on tooth biomechanics: a finite element analysis, Eur. J. Oral Sci. 124 (2016) 591-596. https://doi.org/10.1111/eos.12303.

[39] M.A. Versiani, A. Keleş, Applications of micro-CT technology in endodontics, in: K. Orhan (Ed.), Micro-computed Tomography (Micro-CT) in Medicine and Engineering, Springer Nature, Switzerland, 2020, pp. 183-211. https://doi.org/10.1007/978-3-030-16641-0_12.

[40] A. Keleş, C. Keskin, R. Alqawasmi, M.A. Versiani, Evaluation of dentine thickness of middle mesial canals of mandibular molars prepared with rotary

instruments: a micro-CT study, Int. Endod. J. 53 (2020) 519-528. https://doi.org/10.1111/iej.13247.

[41] M.A. Versiani, K.K.T. Carvalho, J.F. Mazzi-Chaves, M.D. Sousa-Neto, Micro-computed tomographic evaluation of the shaping ability of XP-endo shaper, iRaCe, and EdgeFile systems in long oval-shaped canals, J. Endod. 44 (2018) 489-495. https://doi.org/10.1016/j.joen.2017.09.008.

Figures:

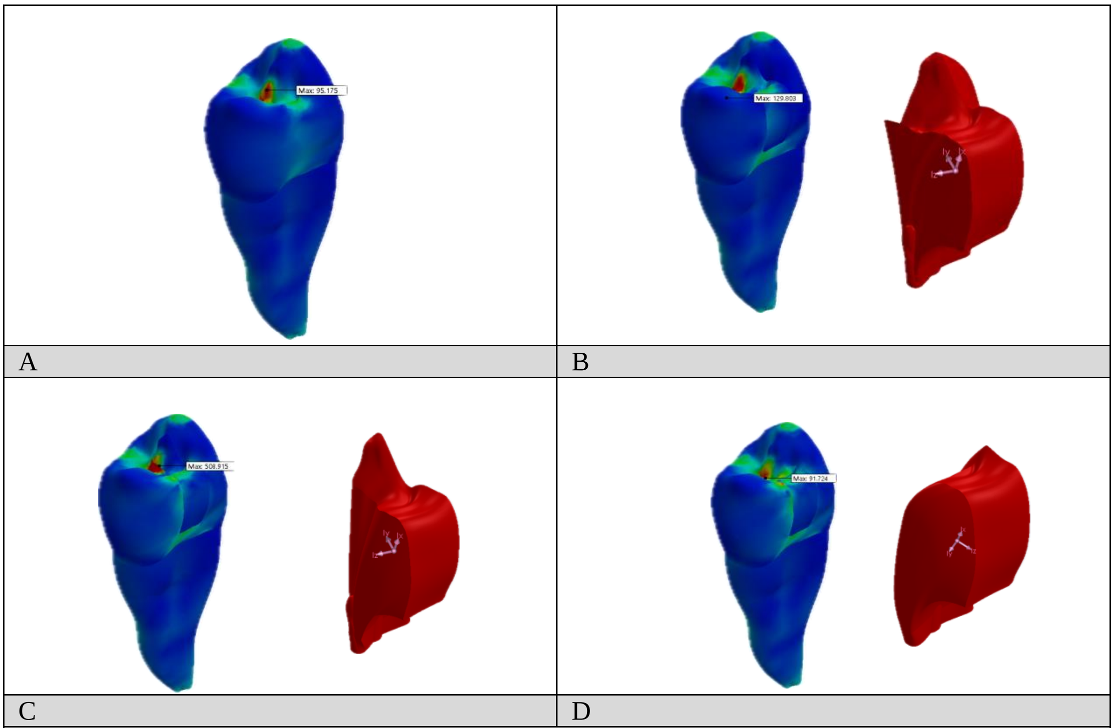

Figure 1: Three-dimensional finite element models of the mandibular second premolar under different access cavity designs. (A) Intact tooth model (IT); (B) Traditional access cavity model (TAC); (C) Conservative access cavity model (CAC); (D) Caries-driven access cavity model (CDA).

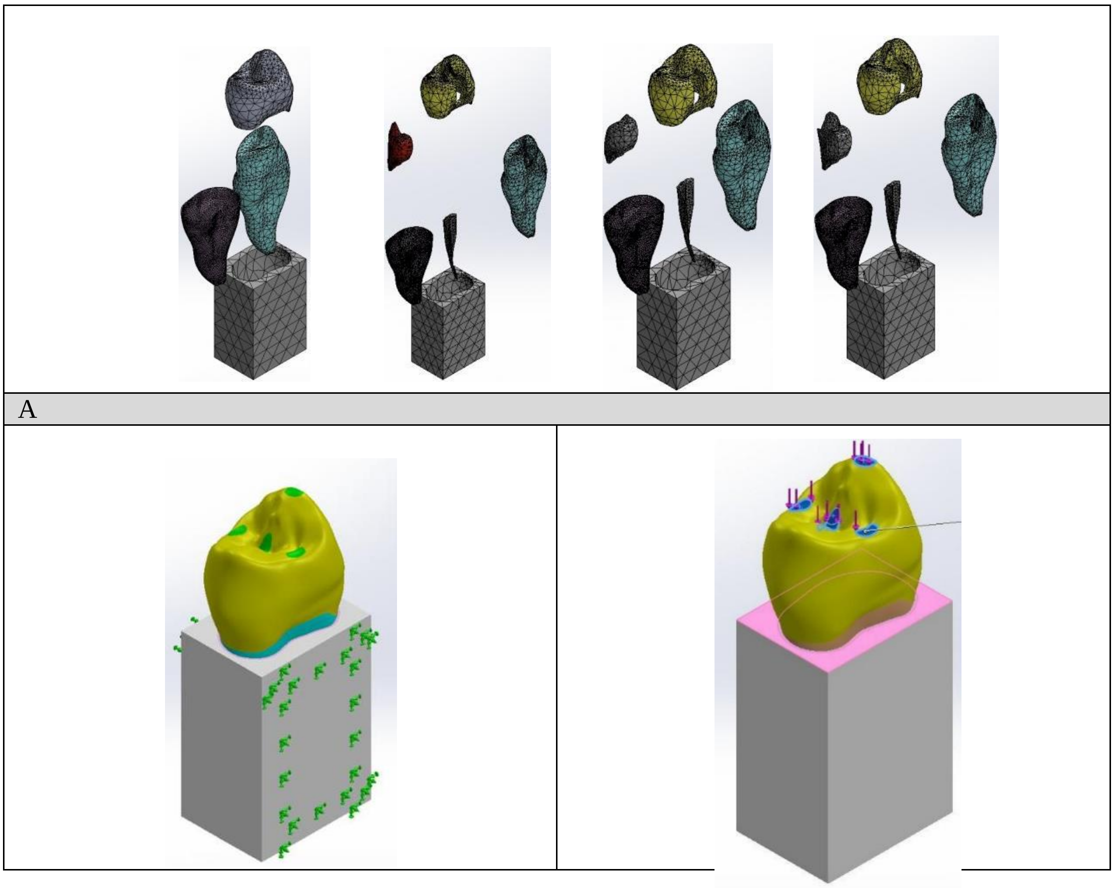

B	C

Figure 2: Finite element analysis setup. (A) Finite element mesh generation and convergence analysis; (B) Fixation of all external surfaces of the alveolar bone in all degrees of freedom; (C) Application of a 200 N static vertical compression force on the occlusal surface.

Group	Solid	TAC	CAC	CDA
CS1	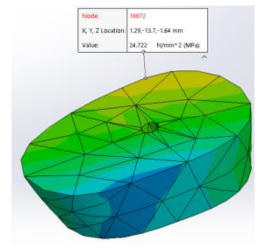	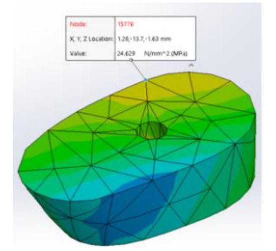	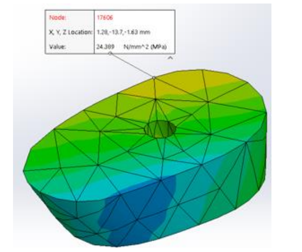	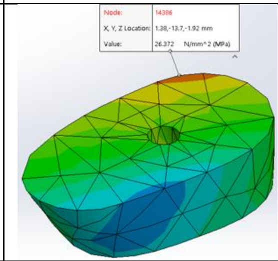
CS2	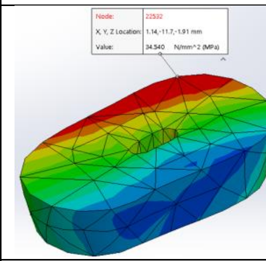	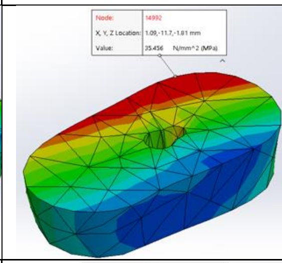	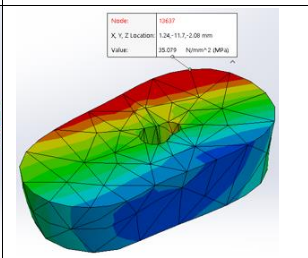	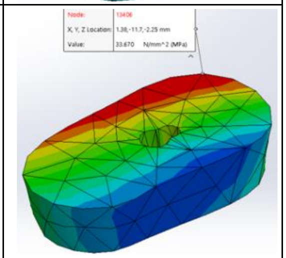
CS3	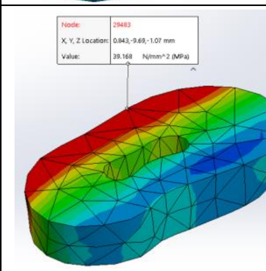	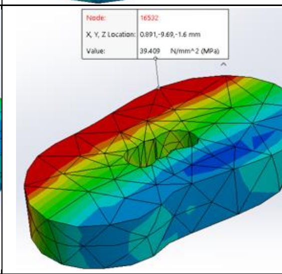	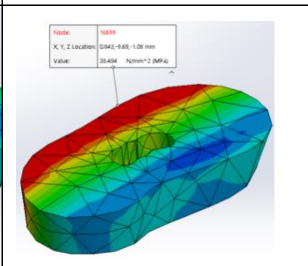	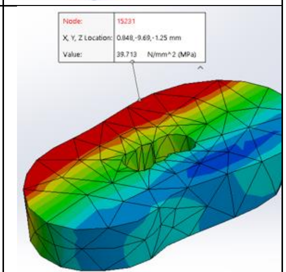
CS4	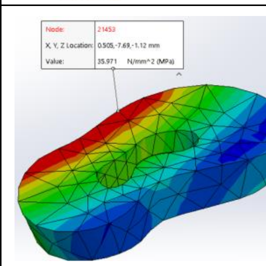	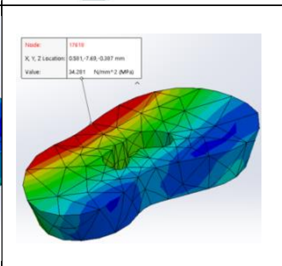	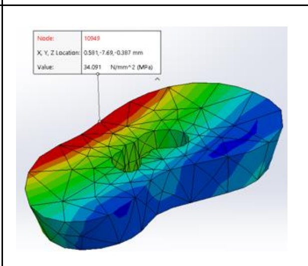	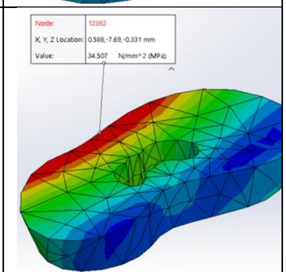
CS5	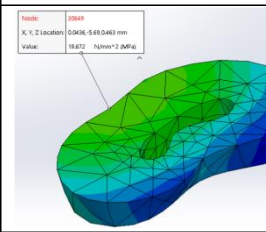	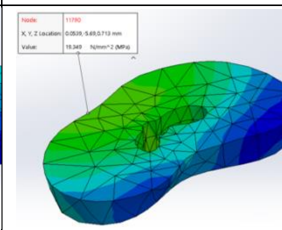	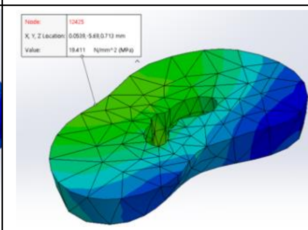	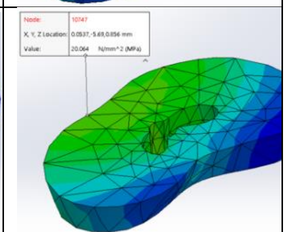
CS6	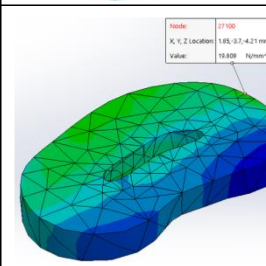	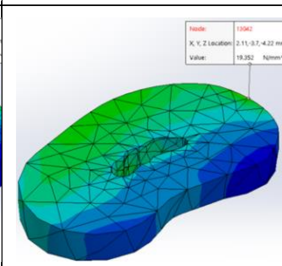	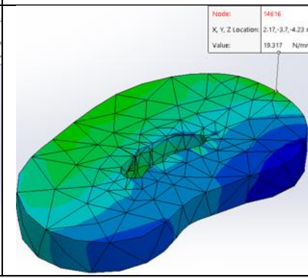	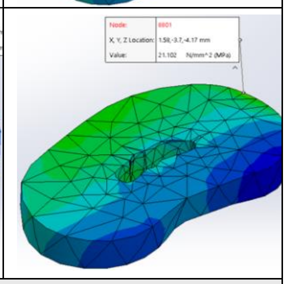

Figure 3: Visual Representation of Von Mises (VM) Stress Distribution (MPa) along Different Root-Level Sections for each Group.